

uvbyCaH β CCD Photometry of Clusters. IV. Solving the Riddle of NGC 3680

Barbara J. Anthony-Twarog¹ and Bruce A. Twarog¹

Department of Physics and Astronomy, University of Kansas, Lawrence, KS 66045-7582

Electronic mail: bjat@ku.edu, twarog@ku.edu

ABSTRACT

CCD photometry on the intermediate-band *uvbyCaH β* system is presented for the open cluster, NGC 3680. Restricting the data to probable cluster members using the CMD and the photometric indices alone defines a sample of 34 stars at the cluster turnoff that imply $E(b - y) = 0.042 \pm 0.002$ (s.e.m.) or $E(B - V) = 0.058 \pm 0.003$ (s.e.m.), where the errors refer to internal errors alone. With this reddening, [Fe/H] is derived from both m_1 and hk using both $b - y$ and $H\beta$ as the temperature indices. The agreement among the four approaches is excellent, leading to final value of [Fe/H] = -0.14 ± 0.03 for the cluster and removing the apparent discrepancy between the past *uvby* analyses and extensive results from the red giants. The primary source of the photometric anomaly appears to be a zero-point offset in the original m_1 indices. Using the homogenized and combined V , $b - y$ data from a variety of studies transformed to $B - V$, the cluster CMD is compared to NGC 752, IC 4651, and the core-convective-overshoot isochrones of Girardi et al. (2002). By interpolation to the proper metallicity, it is found that the $E(B - V)$, (m-M), and age for NGC 752, IC 4651, and NGC 3680 are (0.03, 8.30, 1.55 Gyr), (0.10, 10.20, 1.7 Gyr), and (0.06, 10.20, 1.85 Gyr), respectively. The revised age and metallicity sequence and the color distribution of the giants provide evidence for the suggestion that the giants defining the apparent clump in NGC 3680 are predominantly first-ascent giants, as indicated by their Li abundance, while the clump stars in NGC 752, 0.1 mag bluer in $(B - V)$, are He-core-burning stars. When combined with the color distribution in IC 4651, it is suggested that over this modest age range where He-core flash becomes important, the distribution of so-called clump stars switches from being dominated by He-core burning stars to first-ascent giants in the bump phase.

Subject headings: Galaxy: open clusters and associations:individual (NGC 3680) – techniques: photometric – stars: evolution

1. INTRODUCTION

This is the fourth paper in an extended series detailing the derivation of fundamental parameters in star clusters using precise intermediate-band photometry to identify probable cluster members and to calculate the cluster's reddening, metallicity, distance and age. The initial motivation for this study was provided by Twarog et al. (1997), who used a homogeneous open

cluster sample to identify structure within the galactic abundance gradient, structure that has been corroborated most recently through the use of Cepheids by Andrievsky et al. (2002a,b); Luck et al. (2003), though the origin and reason for the survival of the feature remains elusive (Corder & Twarog 2001; Mishurov et al. 2002; Lépine et al. 2003).

Detailed justifications of the program and the observational approach adopted have been given in previous papers in the series (Anthony-Twarog & Twarog 2000a,b; Twarog et al. 2003) (hereinafter referred to as Papers I, II, and III) and will not

¹Visiting Astronomer, Cerro Tololo Interamerican Observatory. CTIO is operated by AURA, Inc. under contract to the National Science Foundation.

be repeated. Suffice it to say that the reality of the galactic features under discussion will remain questionable unless the error bars on the data are reduced to a level smaller than the size of the effect we are evaluating and/or the size of the sample is statistically enhanced. The overall goal of this project is to do both.

The focus of this paper is the intermediate-age open cluster, NGC 3680. By the normal standards of open cluster research, NGC 3680 has been well-studied on a variety of photometric systems, including *BV* (Eggen 1969; Anthony-Twarog et al. 1991a; Kozhurina-Platais et al. 1997), DDO (McClure 1972; Clariá & Lapasset 1983), Washington (Geisler et al. 1991), and *uvbyH β* (Nissen 1988; Anthony-Twarog et al. 1989; Nordström et al. 1996; Bruntt et al. 1999). It has a respectable level of membership information via proper motions (Kozhurina-Platais et al. 1995) and radial velocities (Mermilliod et al. 1995; Nordström et al. 1997). It has also been analyzed using moderate-dispersion spectroscopy (Friel & Janes 1993; Friel et al. 2002) and at high dispersion (Pasquini et al. 2001). It was initially included in the program as a source of standard stars for calibration of the CCD intermediate-band photometry. However, in the study of Twarog et al. (1997), it was exceptional in that the abundance estimates from DDO photometry and moderate-dispersion spectroscopy of the giants both disagreed significantly with the *uvby*-based abundance from stars at the turnoff of the cluster. The giants indicated a cluster with $[\text{Fe}/\text{H}]$ near -0.15 while the turnoff stars produced $[\text{Fe}/\text{H}]$ closer to $+0.1$. Given the large data samples and the small internal errors in the estimates, the difference could not be dismissed as a byproduct of the internal errors. This left three possible solutions:

(a) The *uvby* system is inherently flawed and, for some unknown reason, produces cluster parameters that are distortions of reality. Though one cannot rule this out without an independent means of testing the parameters generated by the *uvby* system for clusters, the extensive applications of the system to field stars over the last 35 years have generated no evidence for such a failure beyond the usual revisions in the calibrations as data on all sides have improved, contrary to the claims of some authors (Pasquini et al. 2001). In particular, for F stars of disk metallicity, the type

found at the turnoff of NGC 3680, the parametric calibrations have been repeatedly tested and revised (Crawford 1975; Schuster & Nissen 1989; Edvardsson et al. 1993) because of the interest in applying the techniques to studies of the chemical and dynamical evolution of the disk.

(b) The cluster giants and dwarfs produce different results because the stars are different; the distribution of elements in the evolved giants has been altered by evolution while the main sequence stars remain pristine samples of the initial cluster abundance. This could be a plausible suggestion in the case of DDO photometry where the metallicity index includes a CN band, but fails to explain the spectroscopic results tied to, among other things, the Fe lines. Moreover, one is faced with the prospect of explaining why this difference appears in no other open cluster for which comparable data are available, in agreement with standard post-main-sequence evolution scenarios for stars of intermediate mass.

(c) The simplest option, given the high internal precision of the data, is that a zero-point error exists within the sample, either in the *uvbyH β* photometry or in the DDO data. The latter case seems less likely since the DDO $[\text{Fe}/\text{H}]$ was derived independent of the spectroscopic data and both agree at a level consistent with what is found for other clusters. To test the possibility of a zero-point problem with the *uvby* data, it was decided to reduce and analyze the cluster as a program object, rather than include it within the calibration of the CCD data.

Section 2 contains new photoelectric observations of stars in the field of NGC 3680 on the *Caby* system, the details of the *uvbyCaH β* CCD observations, and their reduction and transformation to the standard system. In Sec. 3 we discuss the CMD and begin the process of identifying the sample of probable cluster members. Sec. 4 contains the derivation of the fundamental cluster parameters of reddening and metallicity. In Sec. 5, these are combined with broad-band data to derive the distance and age through comparisons with other clusters and with theoretical isochrones while testing the post-main-sequence predictions of the models. Sec. 6 summarizes the status of NGC 3680 in the context of constraining current models of stellar evolution.

2. The Data

2.1. Observations: Photoelectric *Caby*

The *Caby* system was initially defined and developed using traditional photoelectric photometry obtained at a number of observatories, but predominantly CTIO and KPNO, between 1983 and 1996. These observations, primarily of field stars, have been discussed and analyzed in a series of papers (Anthony-Twarog et al. 1991b; Twarog & Anthony-Twarog 1995; Anthony-Twarog et al. 2000) culminating most recently in the definition of the system for Hyades main sequence stars (Anthony-Twarog et al. 2002). In addition to the Hyades, a number of stars were observed in open and globular clusters with the intent of providing internal standards for future CCD work. Included in this sample were 8 stars in the field of NGC 3680, observed with a pulse-counting system equipped with an S-20 photomultiplier on the 1.0 m and 1.5 m telescopes at CTIO between 1989 and 1992. The cluster stars were transformed and reduced with the field stars and should be well tied to the standard system. Details on the reduction and merger of the photometry over a series of nights and runs may be found in Twarog & Anthony-Twarog (1995) and will not be repeated here. Suffice it to say that the V and $(b-y)$ values are on the system of Olsen (1993). A summary of the data for 8 stars is given in Table 1 where the errors refer to the standard error of the mean for each index. The stars will not be used in the calibration of the CCD photometry but will serve, instead, as a check on the reliability of the overall procedure for calibrating the *Caby* CCD system.

2.2. Observations: CCD *wbyCaH β*

The new photometric data for NGC 3680 were obtained using the Cassegrain-focus CCD imager on the National Optical Astronomy Observatory's 0.9-m telescope at Cerro Tololo Interamerican Observatory. We used a Tektronix 2048 by 2048 detector at the $f/13.5$ focus of the telescope, with CTIO's $4'' \times 4''$ *wby* filters and our own $3'' \times 3''$ $H\beta$ and Ca filters. The field size is $13.5'$ on a side. Frames of all seven filters were obtained in both May 2000 and Jan. 2002.

2.3. Reduction and Transformation

Paper I includes a fairly comprehensive description of the steps used to process the data and the procedures by which we merge photometry based on profile-fitting routines to produce average magnitudes and indices of very high internal precision. Presented here is an outline of the steps followed to transform these instrumental indices to standard photometric systems. We observe standard stars selected from the photometry catalogs of Olsen (1983, 1993, 1994) and our own catalog of *Caby* indices, Twarog & Anthony-Twarog (1995); we also observe stars in open clusters that may be used as standards each photometric night. The clusters are ideal for determining extinction coefficients for indices other than $H\beta$. Aperture magnitudes are obtained for every standard star in the field or in a cluster, as well as for uncrowded stars in the program cluster fields. Apertures ranged from 8 to 11 pixels centered on the star, surrounded by sky annuli of comparable enclosed area. Following correction for atmospheric extinction and the exclusion of stars with serious crowding, average magnitudes in each bandpass are constructed for all stars. From these, mean indices are constructed for stars in every field on each night and compared to standard values. With these transformation equations, indices constructed from aperture photometry may be transformed to standard values. Because we determine the mean difference between the aperture photometry and the profile-fit-based photometry for each index for the program cluster stars on each photometric night, this calibration may be extended to the averaged profile-fit magnitudes and indices.

On two photometric nights of the January 2002 run, $H\beta$ indices were obtained for stars in NGC 3680 as well as in the following open clusters with standardized $H\beta$ photometry: NGC 2287 (Harris et al. 1993), NGC 2516 (Snowden 1975); NGC 3766 (Shobbrook 1985) and M 67 (Nissen et al. 1987). As the cluster standards cover a broad range of $H\beta$ values, 2.57 to 2.93, they were used to establish the slope of the calibration relation, leaving the determination of the zero point to four field standards from the catalog of Olsen (1983) observed on one of the photometric nights. The standard error of the mean zero-point for the calibration equation is 0.007. NGC 3680 was observed with $H\beta$ filters on one of the photometric nights,

with the mean difference between aperture- and profile-fit-based indices determined with a standard error of the mean of 0.001 mag.

For the hk indices, there are not yet very many open clusters with sufficient standards to supplant the use of field star standards from the catalog of Twarog & Anthony-Twarog (1995). In all, 26 standards were observed on three photometric nights for which $uvbyCa$ frames were obtained. The standards cover a range of over one magnitude in hk , so it was not difficult to use these stars to establish both slope and intercept for the calibration equation; a standard error of the mean of 0.005 mag is associated with the zero-point of the calibration equation. NGC 3680 was observed on two of these photometric nights, permitting determination of the mean difference between aperture and profile-fit hk indices with a precision of 0.004 mag (s.e.m.).

Open cluster stars and field stars observed on three photometric nights of the January 2002 run form the basis of the calibration to standard $uvby$ indices. The open cluster standards were drawn from stars observed by Harris et al. (1993) in NGC 2287, by Shobbrook (1985) in NGC 3766, and by Nissen et al. (1987) in M 67. In addition, 23 field stars were observed over the three nights, several of them giants with photometry from Olsen (1993). Stars in common between the nights among the field star standard sets and among the open clusters were used to map the three nights into a single homogeneous set. As NGC 3680 was also observed on two of these photometric nights, it was straightforward to extend the calibrations to the aperture photometry in NGC 3680, and further to the profile-fit photometry.

As before, the cluster standard sets were used to establish the slopes of the relations between instrumental V , $(b - y)$, m_1 and c_1 , except that insufficient red giant stars were available in the cluster standard sets to determine the distinct slopes and color terms for the m_1 and c_1 relations; for these transformations, the cooler field giants were exclusively used. Finally, the 23 field stars were entirely depended upon to set the zero-points of the calibration equations. We estimate the standard errors of the mean zeropoints for the dwarf calibration equations applied to NGC 3680 photometry for V , $b - y$, m_1 and c_1 to be 0.006,

0.006, 0.009 and 0.010; comparable values for the cool giant calibration equations are 0.010, 0.008, 0.010, and 0.017. The remaining contribution to the zero-point uncertainty for the NGC 3680 photometry arises from the determined mean difference between aperture-based indices and profile-fit-based indices; comparisons from two nights on which NGC 3680 was observed suggest that these corrections may be applied to the V , $b - y$, m_1 and c_1 indices with precisions of 0.004, 0.006, 0.008 and 0.008 mag respectively, based on the s.e.m. for the mean index differences.

Final photometric values are found in Table 2, where the primary identification and coordinate description follow the WEBDA database conventions for this cluster as of July 2003. Following each of the six photometric indices are the standard errors of the mean for each index and a summary of the number of frames in each of the seven bandpasses. Stars for which the m_1 and c_1 instrumental indices were transformed using the giant calibration are indicated by brackets around the indices. Stars with $V \lesssim 11.8$ or $m_1 \gtrsim 0.25$ were reduced as giants, as were stars with $b - y \gtrsim 0.46$ and $m_1 \gtrsim 0.2$. These criteria were established by examination of the known giants in the instrumental m_1 , c_1 diagram. Fig. 1 shows the standard errors of the mean for each index as a function of V .

2.4. Comparison to Previous Photometry

Though photometric indices on the $uvbyH\beta$ system have been published on a number of occasions for NGC 3680, the critical comparison is with the data of Nissen (1988) since it has served as a source of local standards for many of the surveys. Of the 33 stars with photoelectric $uvby$ photometry, three (1,3,60) were either outside the limits of the survey or close enough to the edge to lack a sufficient number of frames in b and/or y . Two of the stars (30,80) were excluded because it has been demonstrated in past analyses that they are optical doubles with anomalous indices as defined in Nissen (1988). The residuals in the comparisons between our data and that of Nissen (1988), in the sense (ATT-NI), are $+0.014 \pm 0.010$, 0.007 ± 0.006 , -0.019 ± 0.012 , and -0.012 ± 0.019 for V , $b - y$, m_1 , and c_1 , respectively, from 28 stars. The errors quoted are standard deviations for a single star. The residuals for $H\beta$, -0.008 ± 0.008 ,

are based upon only 8 stars. Generally, the offsets between the indices are modest, with small scatter, particularly in $b - y$. The largest differential, however, is that for m_1 , with the indices of Nissen (1988) being 0.019 mag larger, consistent with a larger implied metallicity; we will return to this point in Sec. 4. The scatter in c_1 is somewhat larger than expected, but is dominated by two of the fainter stars in the sample near $V \sim 14.5$. If these two stars are excluded, the scatter among the remaining 26 stars becomes 0.015 mag.

For *Caby*, the comparison between seven stars from Table 1 that overlap with Table 2, in the sense (Table 2 - Table 1), produces residuals of -0.004 ± 0.008 , -0.001 ± 0.005 , and $+0.007 \pm 0.006$ for V , $b - y$, and hk , respectively. The importance of this small sample is that it is dominated by redder stars well beyond the color limits of the Nissen (1988) survey and thus provides a check on the V and $b - y$ data at the redder end of the scale, while testing the zero-point of the hk indices. It is clear from the small offsets and the scatter in the residuals that, particularly for the cooler stars, the CCD data are in very good agreement with the standard system. If any correction were applied, the CCD hk indices might be reduced by a few millimagnitudes.

More extensive comparisons are available for V and $b - y$ from three CCD surveys. In the discussion that follows, we will make our comparisons first using only stars brighter than $V = 15$, then with all stars brighter than $V = 17.0$. The brighter stars are crucial because the majority of the cluster members lie above this cut and it is more effective to check for color terms among the residuals if the photometry under discussion has small internal errors.

The survey by Anthony-Twarog et al. (1989) (hereinafter referred to as ATS) was among the earliest attempts to study clusters with intermediate-band photometry using CCD's and followed up on analyses of M67 (Anthony-Twarog 1987a), NGC 6397 (Anthony-Twarog 1987b), and IC 4651 (Anthony-Twarog & Twarog 1987). Such programs were plagued by CCD's with small fields of view, high readout noise, and low sensitivity in the blue and ultraviolet, but still provided photometric indices of high internal precision. Four fields were observed in NGC 3680 with only minimal overlap between two of them. Though the

V and $b - y$ zero-points within the fields were set using the data of Nissen (1988), color terms for the entire $b - y$ range from the turnoff to the giants were derived from external standards developed within IC 4651, guaranteeing that the $b - y$ colors were on the standard system, a point possibly missed by Nordström et al. (1996) whose photometry suffers from significant color terms.

Before the comparisons are made, corrections are in order for three stars. The photometry listed for star 84 (ATS ID 2028) is actually that for 83 (ATS ID 2027). The photometry published for 83 should undoubtedly be that for 84, but the indices are clearly not plausible. It is likely that the proximity of stars 83 and 84 is the source of the distortion. Likewise, the indices for star 20 are incorrect and may be related to the fact that it is the brightest star within the observed fields and the image suffered from the effects of near saturation. Stars 20 and the correct 84 will be excluded from the comparison. As summarized in Table 3, for 43 stars with $V \leq 15$, the mean differences in $b - y$ and V , in the sense (Table 2 - ATS), are $+0.007 \pm 0.013$ and $+0.010 \pm 0.013$, in excellent agreement with the comparison to Nissen (1988), as expected. If we expand the sample to all stars $V \leq 17$, we need to exclude only star ATS 2054 which exhibits large residuals in both V and $b - y$. It should be emphasized that this star also has exceptionally large error bars (~ 0.1 mag) for its apparent magnitude in the original survey by Anthony-Twarog et al. (1989). For the remaining 79 stars, the offsets in $b - y$ and V are $+0.004 \pm 0.026$ and $+0.005 \pm 0.023$, respectively. No color dependence is found among the residuals.

A more extensive survey with larger-format CCD's was carried out by Nordström et al. (1996), who used only the photometry of Nissen (1988) to standardize their data. As shown in Table 3, from 86 stars brighter than $V = 15$, the mean residuals in $b - y$ and V are $+0.017 \pm 0.019$ and $+0.020 \pm 0.022$, respectively. However, closer examination reveals a significant correlation of the residuals in V and $b - y$ with $b - y$. If one corrects for this effect using the coefficients in Table 3, the dispersions in the residuals reduce to ± 0.010 and ± 0.017 for $b - y$ and V , respectively. For the sample with $V \leq 17$, two stars with excessive residuals, 511 and 527, are excluded. For the remaining 200 stars, the mean offsets are $+0.016$

± 0.023 and $+0.029 \pm 0.029$ in $b - y$ and V , but virtually identical color corrections emerge from the sample. With the color terms included, the scatter reduces to ± 0.019 and ± 0.026 .

The most recent attempt to use CCD intermediate-band photometry to probe the nature of NGC 3680 is that of Bruntt et al. (1999). From 61 stars brighter than $V = 15$, with no stars excluded, the offsets are $+0.006 \pm 0.013$ and $+0.014 \pm 0.018$ for $b - y$ and V , respectively. No color dependence is found, as expected, since Bruntt et al. (1999) used standards over a wider range of color to transform their indices. The color term in Nordström et al. (1996) was previously noted by Bruntt et al. (1999). Expanding the analysis to all stars, with no exclusions, the offsets become $+0.005 \pm 0.030$ and $+0.025 \pm 0.032$ for $b - y$ and V , respectively.

In summary, for the brighter stars, all three surveys exhibit impressively small scatter in the residuals when compared with Table 2 for both V and $b - y$. After correcting for color terms, the $b - y$ data of Nordström et al. (1996) are a tight match to the current study, with Anthony-Twarog et al. (1989) and Bruntt et al. (1999) only slightly worse. The same trend generally applies for all stars with $V \leq 17$, though the dispersions in the data of Bruntt et al. (1999) at the fainter end are noticeably worse than the other two studies.

3. The Color-Magnitude Diagram: Thinning the Herd

Since one of the primary goals of this investigation is to test the analysis procedure for selecting probable single-star members using a cluster with reliable membership information, we will treat the data for NGC 3680 as if the cluster were a program object comparable to NGC 6253 (Paper III). This means that we will defer making use of the considerable body of data bearing on the membership and binarity of stars in NGC 3680 until after selection on photometric grounds has been attempted.

The CMD for all stars with at least 2 observations each in b and y is presented in Fig. 2. Open circles are the 182 stars with standard errors in the mean for $b - y \leq 0.010$ mag. The morphology of the CMD is identical to that found in the previous intermediate and broad-band CMD's: the cluster is clearly of intermediate age with a well-

defined red giant clump and red hook at the main sequence turnoff. Below $V \sim 15$, the identifiable main sequence becomes lost amid the increasing contamination by field stars.

To minimize potential contamination of the sample in the analysis of the turnoff, our first cut will eliminate all stars with V fainter than 15.0, $b - y$ greater than 0.40, and photometric uncertainty in $b - y$ greater than 0.011 mag. This reduces the sample to the 45 stars plotted in Fig. 3. Fortunately, due to its galactic location and bright apparent turnoff, contamination of the restricted CMD by non-members should not be a significant problem for our analysis, so no attempt will be made to restrict the sample a second time by eliminating stars located well away from the cluster core, a procedure that proved invaluable in Paper III.

3.1. Thinning the Herd: CMD Deviants

Given the high precision of the $b - y$ indices and the expected dominance of the cluster sample over the field stars, it is probable that the majority of stars at the cluster turnoff are members, though not necessarily single stars. Below the turnoff one can readily define the likely location of the single-star main sequence, with two distinct groups of stars bracketing the mean relation. The stars to the blue, noted as crosses in Fig. 3, are tagged as probable field stars since no combination of single-star colors in a composite system will move a star blueward of the main sequence CMD. To the red, the band of stars above the main sequence (open triangles) are tagged as probable binaries and/or nonmembers. Because of evolution off the main sequence, the binary sequence at some point crosses and merges with the vertical turnoff, making separation of the two impossible. The bright limit on the identified binary sequence has been defined with this issue in mind.

Despite the high precision of the $b - y$ data, it is reasonable to question some of the classifications of the stars that are located only 3 sigma off the mean relation. Fortunately, the availability of multiple indices makes the selection process much less subjective. To demonstrate, we make use of the filter pair with the largest baseline, $u - y$. For this select sample of 45 stars, the standard error of the mean in c_1 is typically ± 0.007 mag and no star has an uncertainty larger than ± 0.011 mag. The

comparable error in $u-y$ is less than this. The (V , $u-y$) CMD is shown in Fig. 4 and demonstrates the effectiveness of this index. The increased temperature sensitivity of $u-y$ is obvious and allows easier identification of stars that are too blue for their apparent magnitude (field stars) and stars that are too red (binaries and/or field stars). The symbols have the same meaning as in Fig. 3. With one exception, the stars that lie within the binary sequence in the standard CMD have been identified as such from the $u-y$ index. The one exception is easily explained and does not imply that the star is misidentified as a binary. The binaries that isolate themselves significantly from the main sequence are composed of approximately similar stars from the unevolved main sequence. The $u-y$ index for these stars follows a simple relation between effective temperature and color. For single stars in the vertical band at the turnoff, evolution off the main sequence alters the energy distribution by decreasing the relative contribution of the ultraviolet region blueward of the Balmer discontinuity. Thus, c_1 increases as M_V decreases at a given temperature. The declining contribution of the u filter leads to a redder $u-y$ index due to surface gravity effects rather than temperature, making the more evolved stars appear redder than less evolved stars at the same temperature. The result is that the binary sequence will cross the vertical turnoff at a redder and fainter location than in $b-y$. Note also that the $u-y$ data has identified one additional probable field star that lies significantly redward of the main sequence in $u-y$ but only slightly redward in $b-y$. This star is likely to be a background giant or subgiant and will be excluded from the analysis.

Elimination of the stars that scatter blueward in the $u-y$ figure would remove all the fainter scatter to the blue in the standard CMD. Though it is always possible that elimination of these deviants from the analysis will sweep away a few true cluster members, the remaining sample will contain a high percentage of single stars whose structure and evolution are typical of the cluster as a whole. Finally, for consistency with past analyses, we remove two stars that lie brighter and/or blueward of the main sequence turnoff. The positions of these stars in the CMD would classify them as blue stragglers or non-members. Since, by definition, the blue stragglers undergo anomalous evo-

lution, the inclusion of the parameters based upon their indices is subject to question.

4. Fundamental Properties: Reddening and Metallicity

4.1. Reddening

From the sample of 35 stars selected as probable members from the filled circles in Figs. 3 and 4, we remove an additional star that has $H\beta$ indices based upon one observation in one of the filters. For the remaining 34 stars, the standard error of the mean in $H\beta$ is ± 0.004 mag with the largest individual error at ± 0.012 mag. For m_1 , the comparable statistics are ± 0.006 mag for the typical error, with the largest individual value being ± 0.013 mag.

As discussed in Paper I, derivation of the reddening from intermediate-band photometry is a straightforward, iterative process given reliable estimates of $H\beta$ for each star. The primary decision is the choice of the standard relation for $H\beta$ versus $b-y$ and the adjustments required to correct for metallicity and evolutionary state. The two most commonly used relations are those of Olsen (1988) and Schuster & Nissen (1989). As found in Paper I for IC 4651, both produce very similar but not identical results. We have processed the indices for the 34 non-blue-straggler stars through both relations and find $E(b-y) = 0.040 \pm 0.012$ (s.d.) with Olsen (1988) and $E(b-y) = 0.044 \pm 0.011$ (s.d.) with Schuster & Nissen (1989). As a compromise, we will take the weighted average of the two and use $E(b-y) = 0.042 \pm 0.002$ (s.e.m.) or $E(B-V) = 0.058 \pm 0.003$ (s.e.m.) in the analyses that follow.

4.2. Metallicity from m_1

Given the reddening of $E(b-y) = 0.042$, the derivation of $[\text{Fe}/\text{H}]$ from the m_1 index is as follows. The m_1 index for a star is compared to the standard relation at the same color and the difference between them, adjusted for possible evolutionary effects, is a measure of the relative metallicity. Though the comparison of m_1 is most commonly done using $b-y$ as the reference color because it is simpler to observe, the preferred reference index is $H\beta$ due to its insensitivity to both reddening and metallicity. Changing the metallicity of a star will shift its position in the $m_1 - (b-y)$

diagram diagonally, while moving it solely in the vertical direction in m_1 - $H\beta$. Moreover, reddening errors do not lead to correlated errors in both m_1 and $H\beta$. However, as a check on the derived $[Fe/H]$ based upon the $H\beta$ -defined standard relation, we will also derive the cluster abundance using δm_1 as defined relative to a metallicity-adjusted $b - y$, which should produce very similar results for stars near solar metallicity. This procedure is identical to that applied to IC 4651 in Paper I.

The primary weakness of metallicity determination with intermediate-band filters is the sensitivity of $[Fe/H]$ to small changes in m_1 ; the typical slope of the $[Fe/H]/\delta m_1$ relation is 11. Even with highly reliable photometry, e.g., m_1 accurate to ± 0.015 for a faint star, the uncertainty in $[Fe/H]$ for an individual star is ± 0.17 dex from the scatter in m_1 alone. When potential photometric scatter in $H\beta$ and c_1 are included, errors at the level of ± 0.2 dex are common. As noted in previous papers in this series, the success of the technique depends upon both high internal accuracy and a large enough sample to bring the standard error of the mean for a cluster down to statistically useful levels, i.e., below 0.10 dex. Likewise, because of the size of the sample, we can also minimize the impact of individual points such as binaries and/or the remaining non-members, though they will clearly add to the dispersion.

After correcting each star for the effect of $E(b - y) = 0.042$, the average δm_1 for 34 stars is $+0.027 \pm 0.002$ (s.e.m.), which translates into $[Fe/H] = -0.175 \pm 0.026$ (s.e.m.) for our calibration. For the modified $(b - y)$ -based relation, the average δm_1 is $+0.026 \pm 0.002$ (s.e.m.), which translates into $[Fe/H] = -0.168 \pm 0.024$. The zero-point of the calibration has been set to match the adopted value for the Hyades of $+0.12$.

4.3. Metallicity from hk

We now turn to the alternative avenue for metallicity estimation, the hk index. The hk index is based upon the addition of the Ca filter to the traditional Strömgren filter set, where the Ca filter is designed to measure the band-pass which includes the H and K lines of Ca II. The design and development of the $Caby$ system have been laid out in a series of papers discussing the primary standards (Anthony-Twarog et al. 1991b), an extensive catalog of field star

observations (Twarog & Anthony-Twarog 1995), and calibrations for both red giants (Anthony-Twarog & Twarog 1998) and metal-deficient dwarfs (Anthony-Twarog et al. 2000). Though the system was optimally designed to work on metal-poor stars and most of its applications have focused on these stars (Anthony-Twarog et al. 1995; Baird 1996), early indications that the system retained its metallicity sensitivity for metal-rich F dwarfs have been confirmed by observation of the Hyades and analysis of nearby field stars (Anthony-Twarog et al. 2002).

What makes the hk index, defined as $(Ca - b) - (b - y)$, so useful even at the metal-rich end of the scale is that it has half the sensitivity of m_1 to reddening and approximately twice the sensitivity to metallicity changes, i.e., $\delta[Fe/H]/\delta hk = 5.6$. The metallicity calibration for F stars derived in Anthony-Twarog et al. (2002) used δhk defined relative to $b - y$ as the temperature index. To minimize the impact of reddening on metallicity, this calibration was redone in Paper III using $H\beta$ as the primary temperature index, leading to the relation

$$[Fe/H] = -3.51\delta hk(\beta) + 0.12$$

with a dispersion of only ± 0.09 dex about the mean relation. Though the derived zero-point of the relation was found to be $+0.07$, it has been adjusted to guarantee a Hyades value of $+0.12$, the same zero-point used for the m_1 calibration.

We have derived the cluster metallicity using the hk indices for the same 34 stars analyzed above using both hk relative to the $b - y$ relation and hk relative to $H\beta$. The results relative to $(b - y)$ and $H\beta$ are $[Fe/H] = -0.137 \pm 0.023$ (s.e.m.) and -0.105 ± 0.016 (s.e.m.), respectively.

The unweighted average of the four determinations is $[Fe/H] = -0.146 \pm 0.032$, while inclusion of a weight based upon the inverse of the standard error of the mean raises the average to $[Fe/H] = -0.141$. Given that the calibration curves for the m_1 and hk metallicity relations and the photometric zero-points for the m_1 and hk photometry were derived independently of each other, we find that the cluster metallicity is reasonably well determined at $[Fe/H] = -0.14 \pm 0.03$ (s.e.m.). The agreement between the abundances from m_1 and hk is encouraging in that it is consistent with the revised zero-point for the m_1 photometry. An error of

-0.02 mag in the mean m_1 values would require a correlated error of approximately -0.05 mag in the hk zero-point to ensure that both systems produce similar estimates for $[\text{Fe}/\text{H}]$. It should be noted also that in all four metallicity estimates, a significant portion of the dispersion in $[\text{Fe}/\text{H}]$ arises from 3 of the fainter stars with systematically lower $[\text{Fe}/\text{H}]$ than the cluster mean. Exclusion of these stars would increase $[\text{Fe}/\text{H}]$ by only 0.03 dex, so they will be retained in the analysis.

The impressive precision of the metallicity estimates as characterized by the standard errors of the mean is a product of the small to modest errors for individual stars coupled to a statistically significant sample of members and, thus, refers solely to the internal errors. On the external side, systematic errors may arise at a number of points along the way from processing of the frames to transformation of the instrumental indices to the standard system. Simple propagation of error analyses for the four techniques for defining $[\text{Fe}/\text{H}]$ produce potential systematic uncertainties of ± 0.13 , 0.13, 0.10 and 0.06 dex from the $m_1(b-y)$, $m_1(\text{H}\beta)$, $hk(b-y)$, and $hk(\text{H}\beta)$ $[\text{Fe}/\text{H}]$ determinations, respectively. Given the weighted average of the final values, the best estimate for the external error in the derived value of $[\text{Fe}/\text{H}]$ is just under 0.10 dex.

4.4. Comparison to Previous Determinations

For the reddening, there are a significant number of determinations, though not all are independent. The first reddening estimate of $E(B-V) = 0.04$ by Eggen (1969) was based upon interpolation of the cluster distance relative to 3 early-type stars in the cluster field with $E(B-V)$ derived from BV photoelectric photometry and spectral types. McClure (1972) challenged the reliability of this approach and obtained $E(B-V) = 0.09$ from DDO photometry of 8 red giant members of the cluster. Janes (1979) revised the DDO estimate using an updated photometric approach to obtain $E(B-V) = 0.06$, but an additional DDO survey by Clariá & Lapasset (1983) found $E(B-V) = 0.10$. The DDO approach was revisited by Twarog et al. (1997) where the combined photometry of McClure (1972) and Clariá & Lapasset (1983) generated $E(B-V) = 0.095$ with the calibration of Janes (1977).

A potential weakness of the early DDO results

is that they required $B-V$ colors; regular use was made of the Eggen (1969) photoelectric data. Comparisons with more recent photoelectric observations in the cluster (Anthony-Twarog et al. 1991a; Kozhurina-Platais et al. 1997) indicate that the Eggen (1969) $B-V$ values for the giants may be 0.01 to 0.02 mag too red. Correction for this small shift in the relation used by McClure (1972) would lower the DDO estimate by between 0.02 and 0.04 mag and the other estimates by slightly smaller values. It should be noted that the four stars classified as photometric non-members from the DDO data are now known to be non-members from both proper-motion and radial-velocity work, while all 8 stars included in the DDO analyses are members.

Among the giants, Eggen (1983) found $E(B-V) = 0.05$ using a modified Strömgen system combined with RI photometry, but later revised the calibration to find $E(B-V) = 0.095$ (Eggen 1989). Though the issue of binarity in 3 of the 8 giants has been raised in the past, exclusion of these stars from the average has no significant statistical impact on the cluster mean.

For the turnoff stars, $uvby\text{H}\beta$ data imply $E(b-y) = 0.034$ from 8 stars (Nissen 1988), 0.031 from 3 single-star members (Nordström et al. 1997), and 0.048 from 11 single-star members (Bruntt et al. 1999). The higher value of Bruntt et al. (1999) is surprising since their photometry is tied to the system of Nissen (1988) and they derive the reddening with the same relation. In all three cases, the derived $[\text{Fe}/\text{H}]$ is approximately $+0.1$; lowering the metallicity by 0.2 dex should lead to a higher $E(b-y)$ by about 0.01 mag due to the expected bluer intrinsic colors. Such a correction would bring Nissen (1988) and Nordström et al. (1997) into excellent agreement with the value derived in this investigation. Note that our slightly redder indices for both $(b-y)$ and $\text{H}\beta$ relative to Nissen (1988) cancel out in the reddening determination.

Two more indirect estimates should be mentioned. Kozhurina-Platais et al. (1997) optimized a match between the cluster CMD and solar metallicity isochrones to derive $E(B-V) = 0.075$. The reddening maps of Schlegel et al. (1998) indicate $E(B-V) = 0.094$ in the direction of NGC 3680, an upper limit along this line of sight and surely higher than the cluster value. In summary, given

the uncertainty inherent in all of these techniques, there appears to be no significant discrepancy with the value of $E(B - V) = 0.06$ derived from our *uvby*H β photometry of the probable cluster members at the turnoff.

The metallicity estimates for the cluster have fallen into two distinct camps. Prior *uvby*H β photometric estimates at the turnoff have been linked to the study by Nissen (1988) and have generated numbers virtually identical with the original estimate of $[\text{Fe}/\text{H}] = +0.09$: $+0.10$ (Anthony-Twarog et al. 1989), $+0.11$ (Nordström et al. 1997), and $+0.09$ (Bruntt et al. 1999). In contrast, every recent analysis of the giants, photometric and spectroscopic, has elicited values between -0.10 and -0.20 . The homogenized DDO photometry of the member giants has been discussed by Twarog et al. (1997) using the revised calibration of Twarog & Anthony-Twarog (1996) and gives $[\text{Fe}/\text{H}] = -0.12$; the result does not change if the binaries are excluded. The reddening adopted in that discussion was $E(B - V) = 0.05$. The moderate-dispersion spectroscopic work of Friel & Janes (1993), updated and expanded by Friel et al. (2002), produces $[\text{Fe}/\text{H}] = -0.19$ for 6 member giants on a scale that is typically 0.05 to 0.1 dex more metal-poor than the revised DDO scale. The mean value remains unchanged if the 2 binary giants are excluded. The lower metallicity of the giants has also been corroborated by a high-resolution spectroscopic sample of 6 giants by Pasquini et al. (2001), who find $[\text{Fe}/\text{H}] = -0.17$ on a scale where the Hyades is $+0.13$; the mean remains unchanged if the 2 binaries are excluded. Finally, Washington photometry of the giants by Geisler et al. (1991) leads to $[\text{Fe}/\text{H}] = -0.14$ on a system where the Hyades has $[\text{Fe}/\text{H}] = +0.07$.

In summary, there is now excellent agreement between the spectroscopic and photometric metallicity of the giants and that of the turnoff stars in NGC 3680 as determined by both the *uvby* and the *Caby* systems. The source of the long-standing discrepancy appears to be a modest zero-point offset in the m_1 indices obtained by Nissen (1988). We cannot overemphasize the fact that this conclusion is not simply a choice of our zero-point over that of Nissen (1988); it is always possible that our zero-point for m_1 is systematically off by 0.01 mag. However, the agreement between m_1 and the more sensitive *hk* index, as well as the extensive

work on the giants, gives us confidence that the true $[\text{Fe}/\text{H}]$ of NGC 3680 is closer to -0.10 than $+0.10$.

4.5. Comparison With Reality

Before discussing the age and distance to the cluster from isochrone fits, it is important to see if our approach to eliminating the deviants from the CMD was successful or an exercise in bias. This can be accomplished because the majority of the stars in our field have proper-motion (Kozhurina-Platais et al. 1995) and radial-velocity (Nordström et al. 1997) data that allows us to determine if they are field stars and/or binaries.

At the faint end of the scale, three stars were removed from the CMD because they were located blueward of the main sequence in both $b - y$ and $u - y$. Stars 1037 and 2024 have only proper-motion data; both are 0% probable members. Star 2095 has both radial-velocity and proper-motion data; it is a non-member. On the red side of the main sequence, 5 stars were removed. Three (22,24,36) are members but spectroscopic binaries; two (16,3064) are non-members. Of the stars near the turnoff, excluded for being too blue and/or too bright, both 57 and 48 are proper-motion and radial-velocity non-members. Thus, every star identified as potentially being a field star or a binary does, in fact, fall within one or both of these categories.

In contrast, of the 34 stars used in the derivation of the cluster parameters, how many are probable non-members? Using the classification by Nordström et al. (1997), 6 of the stars with proper motion and radial-velocity data are likely non-members: 29,31,82,1085,2093, and 3001. Of these, use of the c_1 index would have quickly removed 29. It is located at the top of the turnoff, but has indices indicative of a totally unevolved star. In fact, using the cluster reddening on this foreground star places it below the main sequence in a $c_1 - (b - y)$ diagram. The other five stars, however, have $c_1 - (b - y)$ indices that do not distinguish them from the other cluster stars, single or binary. Surprisingly, the binary star members follow a virtually identical distribution in the $\delta c_1, \delta M_V$ diagram as the single stars. Expectation would be that larger c_1 at a given $(b - y)$ (or H β) would correlate with distance above the unevolved main sequence for single stars; binaries would iso-

late themselves in such a figure by having c_1 for an unevolved star but systematically larger δM_V , an effect seen in analyses of NGC 752 (Twarog 1983; Daniel et al. 1994) and M67 (Nissen et al. 1987). This does not appear to be the case in NGC 3680, despite the high internal accuracy of the photometry.

It's worth noting that the fundamental cluster parameters of reddening and metallicity derived with these six non-members included, are changed only slightly if the non-members are explicitly excluded. The derived reddening, for example, is only 0.001 mag larger with the six non-members excluded. Derived estimates of $[\text{Fe}/\text{H}]$ with the non-members excluded are lower by ~ 0.005 , except for the estimate based on $hk(b - y)$ which drops by 0.02.

We close this comparison by noting that of the six stars classed as non-members, only two, 29 and 2093, are non-members in both radial velocity and proper motion. Star 1085 is a radial-velocity member, but excluded on the basis of proper-motion. The remaining three are 0 probability radial-velocity members, but moderate to high probability proper motion members: 31 (69 %), 82 (49 %), and 3001 (70 %). Star 3001 is a virtual photometric twin for star 10, a similarity that extends to the Li abundance. Star 31 is a photometric twin for 4002; both are classed as SB1 binaries. The Li for star 31 is also consistent with its location in the CMD. Though these similarities may be pure statistical coincidence, it should be remembered that NGC 3680 is a cluster in a state of ongoing dissolution. Based upon number counts (Anthony-Twarog et al. 1991a), proper motions (Kozhurina-Platais et al. 1995), and radial velocities (Nordström et al. 1997), it has been known for some time that NGC 3680 suffers from a deficiency of lower main sequence stars, i.e., those with M_V greater than 5. Since there is every reason to believe that the cluster formed with such stars, their absence is an indication that dynamical evaporation has been a key process defining the current appearance of the cluster. By extension, the process is no doubt continuing and, at any given point in time, some stars that formed with the cluster should be in the transition state between gravitationally bound and unbound. Thus, the similarities between stars that are technically non-members and those that meet both velocity

criteria may not be purely coincidental. In short, inclusion of these three stars would have had no significant impact on the determination of its parameters since they are virtual twins to stars that are cluster members.

5. Fundamental Parameters: Distance and Age

5.1. The Broad-Band CMD - Transforming the Data

Given the reddening and metallicity, the traditional approach to deriving the distance and age is to compare the cluster CMD to a set of theoretical isochrones for which the color transformations and bolometric corrections between the theoretical and the observational plane reproduce the colors and absolute magnitudes of nearby stars with known temperatures and abundances. From an age standpoint, the critical test is whether or not a star of solar mass, composition, and age resembles the sun. For open clusters of solar and sub-solar abundance, the impact of this issue on cluster ages and distances has been emphasized on a variety of occasions (Twarog & Anthony-Twarog 1989; Twarog et al. 1993; Daniel et al. 1994; Twarog et al. 1995, 1999).

As we have noted in past analyses, isochrones are invariably created for broad-band systems and a check of the most recent publications shows that the theoretical isochrones are available on the *UBVRI* system, among others, but not for *wvby*. This problem has been solved in the past by making use of the fact that $b - y$ is well correlated with $B - V$ at a given $[\text{Fe}/\text{H}]$ with little dependence on evolutionary state. In contrast with most clusters, however, there is a wealth of $b - y$ CCD and photoelectric data for NGC 3680 but only one precise CCD *BV* survey. The early *BV* work of Eggen (1969) has been called into question when compared to more recent data (Anthony-Twarog et al. 1989; Nordström et al. 1996) and the photographic data of Anthony-Twarog et al. (1989), though consistent within a zero-point shift for the stars $V \leq 15$, has larger photometric scatter than one would like. Thus, the only reliable *BV* study with high internal precision is that of Kozhurina-Platais et al. (1997), which only includes independent photometry for 143 probable members (data for 3 stars are taken from other surveys.)

To maximize the internal accuracy, the five *by* surveys to date, (Nissen 1988; Anthony-Twarog et al. 1991a; Nordström et al. 1996; Bruntt et al. 1999) and this study, have been merged. The photometry of Table 2 has been adopted as the standard system and each sample, including the photoelectric *Caby* data of Table 1, has been transformed to the standard system using the offsets/linear relations calculated in Sec. 3.3. Stars noted as deviants in each survey have been excluded unless otherwise noted below. All stars with $V \leq 15$ have been included in the merger, though the data from Nissen (1988); Nordström et al. (1996) and the current investigation have been given twice the weight of the remaining studies. For $V > 15$, only the stars in Nordström et al. (1996) and Table 2 have been merged.

To locate potential problems, all stars with standard deviations in V and/or $b-y$ greater than 0.03 mag have been identified. For V , 14 stars meet the criteria, but 6 have $V \geq 16$. The remaining 8 stars are 47, 51, 60, 84, 86, 2060, 4015, and 4104. For $b-y$, only 9 stars meet the criteria, and 6 of these are have $V \geq 16$. The remaining problems are 51, 60, and 2060. With the exception of star 51, the errors in V , if real, would not seriously impact the position of the star in the CMD while the errors in color would since they translate into a $B-V$ shift of 0.07 to 0.10 mag. For the V mag, we can call upon three broadband surveys to identify the probable source of the problem: the CCD data of Hawley et al. (1999); Kozhurina-Platais et al. (1997), and the photoelectric data of Anthony-Twarog et al. (1991a). For each of these studies, the mean offsets in V , in the sense (Table 2 - ref), are found to be $+0.033 \pm 0.017$ (s.d.) from 90 stars (Hawley et al. 1999), $+0.020 \pm 0.012$ from 82 stars (Kozhurina-Platais et al. 1997), and -0.017 ± 0.019 from 19 stars (Anthony-Twarog et al. 1991a). In each comparison, stars that deviated from the mean residual by more than 0.05 mag were excluded from the mean. We note that past comparisons to the photoelectric data of Anthony-Twarog et al. (1991a) have often exaggerated the uncertainty in this photometry by including the poorly calibrated CCD data with the brighter photoelectric data. It is undoubtedly the case that the attempt to extend the photographic calibration to fainter magnitudes using the CCD observations is a primary source of

the non-linear residuals seen in the fainter photographic photometry.

In the case of star 51, our CCD processing finds 2 stars at the expected position, identified as 51A ($V = 15.16$) and 51B ($V = 15.58$) in Table 2. Most surveys find $V \sim 14.65$, though Bruntt et al. (1999) finds $V = 14.87$. Because of the potential composite nature of this star, it will be excluded from further discussion. For 2060, Table 2 gives $(V, b-y) = (15.784, 0.511)$ with no significant variation in the indices. Bruntt et al. (1999) and Nordström et al. (1996) find almost identical values of $(15.695, 0.62)$ while Hawley et al. (1999) find $V = 15.79$. Since this star is a non-member, it will be excluded from further discussion. For star 60 the situation is more complicated since it is classified as a probable cluster member. In V , there is no clear pattern of variation with 5 studies providing an almost uniform distribution of values from 14.256 to 14.318; we will adopt 14.29 as a compromise. The significant variation is in the color. Using the $b-y, B-V$ transformations derived below, the $B-V$ index implied or directly observed for the star ranges from 0.536 (Bruntt et al. 1999) and 0.586 (Anthony-Twarog et al. 1991a) to 0.639 (Kozhurina-Platais et al. 1997) and 0.642 (Nissen 1988). As a compromise, we will adopt $b-y = 0.40$ and $B-V = 0.60$ for the star, noting that it may be a variable.

The next step in the procedure is the transformation from $b-y$ to $B-V$. Using the BV data of Kozhurina-Platais et al. (1997) as the standard system, linear relations were derived between $b-y$ and $B-V$, breaking the sample into blue and red stars to account for the likelihood of a slope change between the two color ranges. For the red stars, the fit was also repeated using only stars brighter than $V = 15.0$, with no significant change found in the relation compared to the entire sample. The final adopted transformations are:

$$b-y \leq 0.32$$

$$B-V = 1.346(\pm 0.035)*(b-y) + 0.025(\pm 0.011)$$

$$(b-y) > 0.32$$

$$B-V = 1.777(\pm 0.014)*(b-y) - 0.115(\pm 0.009)$$

The standard deviations of the residuals about the mean relation for the regions are ± 0.008 for the 29 bluer stars and ± 0.012 for the 46 redder stars $V \leq 15$.

To ensure optimal photometry on the standard BV system for all the stars, particularly the giants, two additional comparisons were made. Anthony-Twarog et al. (1991a) published photoelectric data for 28 stars that were used in conjunction with CCD frames to calibrate the photographic survey. Though the attempt to extend the calibration to fainter stars proved flawed, the photoelectric data were reasonably well tied to the standard BV system. Comparing the photoelectric data to the composite by data transformed to $B - V$, from 20 stars one finds the residuals in V and $B - V$, in the sense (CCD-PE) to be -0.017 ± 0.019 and 0.000 ± 0.025 , respectively. If one unusually deviant star, 4095, is excluded, the average residual in $B - V$ becomes -0.004 ± 0.016 .

Photoelectric data on the Geneva system has also been published by Mermilliod et al. (1995) for 10 redder stars. Assuming the $[B-V]$ listed for star 13 in their Table 1 is an error and should read 0.493, we have transformed the Geneva index to $B - V$ using the relation provided by Mermilliod et al. (1995). The residuals in V and $B - V$ from 9 stars relative to the transformed by data, in the sense (CCD - ME), are 0.014 ± 0.014 and 0.005 ± 0.022 , respectively. If the one star exhibiting anomalous residuals, star 34, is excluded, the revised residuals become 0.010 ± 0.005 and -0.001 ± 0.015 , respectively.

In addition to demonstrating that the $B - V$ data are on the standard system, we can combine the results for star 53, the only giant not observed in the by sample, from the 3 surveys to minimize the impact of any potential problem in the data of Kozhurina-Platais et al. (1997). Using the revised offsets, the final V and $B - V$ values for this star are found to be 10.879 ± 0.036 (s.d.) and 1.120 ± 0.012 (s.d.) from 3 measurements. The error in V is larger than one would like, but will have a negligible impact on the position of the star in the CMD.

5.2. The CMD Fit: NGC 752

With the cluster BV photometry available, the usual procedure would be to compare the reddening-corrected CMD to a set of appropriate isochrones and derive the age and distance. Instead, we will compare NGC 3680 to the observational data for NGC 752. The rationale for this is straightforward. With the revised metallic-

ity for NGC 3680, the cluster is identical within the uncertainties to NGC 752. The DDO data and moderate dispersion spectroscopy for NGC 752 combined give $[Fe/H] = -0.09$ from 16 giants (Twarog et al. 1997). The turnoff photometry on the $uvby$ system, transformed to the system of Crawford & Barnes (1970), gives $[Fe/H] = -0.08$ from 31 stars while the photometric zero-point of Twarog (1983) gives -0.20 (Daniel et al. 1994). The reddening estimate for NGC 752 from DDO and $uvby$ photometry combined is $E(B-V) = 0.03$ (Daniel et al. 1994). By comparing NGC 3680 to a real cluster, one avoids the problems inherent in choosing specific theoretical isochrones tied to different color transformations and differences in the adopted internal physics.

To superpose the clusters, we must apply differential shifts in color and apparent magnitude to account for the reddening differential and the difference in the apparent modulus. For the color shift, we decrease the $B - V$ colors of the stars in NGC 3680 by 0.03 mag. For the ΔV , we use the distribution of giants, in particular, the red giant clump defined by the concentration of stars undergoing He-core burning prior to their second ascent of the red giant branch. In NGC 752, the clump of stars is easily identified at $V = 9.00 \pm 0.05$. For NGC 3680, the giant distribution shows a strong concentration of stars between $V = 10.85$ and 10.95 ; we adopt 10.90 ± 0.05 as the clump location in NGC 3680, leading to a differential of $\Delta V = -1.90$. The resulting superposition of the two CMD's is shown in Fig. 5. Note that we have included all stars identified as members. Open circles are stars in NGC 752, while asterisks are probable binaries. Filled circles are stars in NGC 3680, with triangles representing the known binaries. We also emphasize that the majority of the photometry in NGC 752 is a composite average of photoelectric data, though some of the fainter stars have solely photographic estimates.

In Fig. 5, the agreement between the turnoff and unevolved main sequences is excellent. The blue edges of the distribution for both clusters, populated by single stars and binaries with mass ratios significantly less than 0.5, superpose at a level such that a differential shift of more than 0.02 mag in $B - V$ in either direction would be readily detectable. The redder and fainter turnoff for NGC 3680 demonstrates the greater age of the

cluster. In contrast, the red giants, while matching up well in V by design, do not superpose at all in $B - V$. The clump in NGC 3680 is almost 0.10 mag redder than in NGC 752. It is impossible to simultaneously match the luminosity and colors for the main sequences and the clumps of stars on the giant branches of the two clusters. Since the primary difference between the two clusters is the greater age of NGC 3680, one option may be that the red giant clump undergoes a significant shift to the red between the age of NGC 752 and NGC 3680. To investigate this option, we turn to the theoretical isochrones.

5.3. The CMD Fit: The Isochrones

There is a variety of isochrone sets available for comparison with broad-band photometry. For consistency with our previous discussion of IC 4651 and because, when properly zeroed to the same color and absolute magnitude scale, most sets produce similar results for ages and distances, we will use the sets of Girardi et al. (2002) (hereinafter referred to as PAD). Moreover, based upon the many comparisons, including our own (Anthony-Twarog et al. 1991a; Daniel et al. 1994; Anthony-Twarog et al. 1994; Twarog et al. 1995), between open clusters and past and present generations of isochrones, we will only make use of isochrones that include convective overshoot mixing. On a scale where solar metallicity is $Z = 0.019$ and $Y = 0.273$, PAD isochrones were also obtained for $(Y, Z) = (0.250, 0.008)$ and $(0.300, 0.030)$ or $[\text{Fe}/\text{H}] = -0.38$ and $+0.20$, respectively. Since isochrones with $[\text{Fe}/\text{H}] = -0.10$ to -0.15 are not available, it was decided to define the cluster parameters assuming each of the three abundances was appropriate and interpolate the results for the derived $[\text{Fe}/\text{H}]$. As a first step, the solar metallicity isochrones were checked to ensure that they were on our adopted color and absolute magnitude scale of $M_V = 4.84$ and $B - V = 0.65$ for a solar mass star at 4.6 Gyrs. A check of the solar metallicity isochrones of PAD shows that they are too red by 0.032 mag in $B - V$ and too bright by 0.02 mag in V . For consistency, these offsets have been applied to all the isochrones used, though there is some evidence that a smaller correction may be more appropriate for the more metal-poor isochrones (Twarog et al. 1999). The impact of such a differential correction on our conclusions is

minor.

With $E(B - V) = 0.03$ and 0.06 for NGC 752 and NGC 3680, respectively, and NGC 3680 offset by -1.90 in V relative to NGC 752, the cluster CMD's were compared to the isochrones by deriving the apparent modulus for NGC 752 that guaranteed a match to the main sequence between $V = 12.5$ and 13.5 . Fig. 6 shows an example of the fit for the solar metallicity isochrones with an apparent modulus, $(m-M)$, of 8.50 and ages of 1.26, 1.41, and 1.58 Gyrs. For $[\text{Fe}/\text{H}] = +0.2, 0.0,$ and -0.38 , the required apparent moduli are 8.80, 8.50, and 7.95, respectively. For NGC 752, the ages are 1.05, 1.30, and 2.15 Gyr while for NGC 3680, the comparable numbers are 1.20, 1.55, and 2.55 Gyrs. It should be emphasized that for the lowest $[\text{Fe}/\text{H}]$, the agreement between the observed and theoretical CMD's at the turnoff is less than ideal; we have defined the ages based upon the color of the bluest point at the turnoff and the location of the red hook relative to the isochrones. Rounding off to the nearest 0.05, interpolation of the values for $[\text{Fe}/\text{H}]$ between -0.10 and -0.15 leads to an apparent modulus for NGC 752 of $(m-M) = 8.30 \pm 0.1$ and, for NGC 3680, $(m-M) = 10.20$. For the ages, we have interpolated in $\log(\text{age})$ relative to $[\text{Fe}/\text{H}]$. For NGC 752 and NGC 3680, the respective ages are 1.55 and 1.85 Gyr, with an approximate uncertainty in both values near 0.1 Gyr.

For NGC 752, this age estimate is in excellent agreement with past values from a variety of isochrone fits. Daniel et al. (1994), using the overshoot models of Schaller et al. (1992) found an age of 1.7 ± 0.1 Gyr. Kozhurina-Platais et al. (1997), using identical reddening and distance modulus, found an age of 1.6 ± 0.2 Gyr using the Yale isochrones (Green et al. 1987; Chaboyer et al. 1992). Given the differences in the models, the overall consistency is more than satisfactory and implies that, when comparable cluster parameters are adopted, the different sets of isochrones zeroed to the same scale should produce similar ages and moduli.

For NGC 3680, the comparisons are more discordant due to the frequent adoption of a higher metallicity for the cluster. Kozhurina-Platais et al. (1997), adopting $E(B - V) = 0.075$ and $(m-M) = 10.45$, find an optimum match for their overshoot parameter for an age of 1.6 Gyr when compared to a solar composition isochrone; our match

to the solar composition models of PAD produces an apparent modulus of 10.40 and an age of 1.55 Gyr. There is every reason to believe that had Kozhurina-Platais et al. (1997) adopted the correct metallicity and a slightly lower reddening, the Yale isochrones would have produced an age and modulus comparable to 1.85 Gyr and 10.20. Exactly the same argument can be made with the results of Nordström et al. (1997) where, assuming $E(B - V) = 0.05$ and Hyades metallicity, $[\text{Fe}/\text{H}] = +0.12$, $(m-M) = 10.65$ and an age of 1.45 Gyr are derived using the isochrones of Schaller et al. (1992). With a slightly higher reddening, our interpolated values for this metallicity are $(m-M) = 10.6$ and 1.35 Gyr, effectively no difference.

We close this section by noting the results for another cluster, IC 4651, the first cluster analyzed in Paper I. Unlike NGC 3680, there is little disagreement regarding the metallicity of IC 4651 from either the main sequence photometry (Anthony-Twarog & Twarog 2000a) or the DDO photometry of the giants (Twarog et al. 1997): the cluster is more metal-rich than the sun and essentially the same as the Hyades within the uncertainties. From *uvby*H β analysis, in Paper I we found that $E(b - y) = 0.071$ or 0.062, depending upon the choice of intrinsic color relations. More important was the comparison between NGC 3680 and IC 4651. On the assumption that the two clusters had the same $[\text{Fe}/\text{H}]$, it was found that the CMD's superposed exactly at the turnoff and on the giant branch if $E(b - y)$ for IC 4651 was larger than that of NGC 3680 by 0.04. Since we now know that NGC 3680 is more metal-poor than IC 4651, the difference caused by reddening alone is reduced to 0.03 mag in $E(b - y)$. With $E(b - y) = 0.042$ for NGC 3680, this implies $E(b - y)$ for IC 4651 of 0.07, thereby favoring the larger value but not inconsistent with the smaller number, given the uncertainties.

Using the range in reddening values ($E(b - y) = 0.062$ to 0.071), the age range and apparent modulus range derived in Paper I were 1.7 to 1.6 ± 0.1 Gyr and 10.15 to 10.3 using the same source of theoretical isochrones adopted above for NGC 3680. The isochrones were transformed directly from the theoretical plane to $b - y$ for a Hyades composition and a direct fit made to the Hyades $V - (b - y)$ main sequence. The age and distance were in excellent agreement with comparable prior analyses based

upon the same metallicity and reddening when use was made of isochrones with convective overshoot. Since then, Meibom (2000) adopted $E(b - y) = 0.076$ and fit the $V - (v - y)$ relation directly to the Hyades to get $(m-M) = 10.36$, identical with the values of Paper I if the same reddenings are selected.

The age values have been corroborated with the same reddening but independent *uvby* photometry by Meibom et al. (2002) and the isochrones of Yi et al. (2002) and Schaller et al. (1992). For $E(b - y) = 0.062$ to 0.071, the isochrones of Schaller et al. (1992) give 1.7 to 1.6 Gyr, while the Yi et al. (2002) isochrones generate ages systematically larger by 0.2 Gyr. It should be noted that the age estimates in Meibom et al. (2002) are heavily weighted by the few points identified as single stars from radial-velocity work and that the turnoff region in $b - y$ shows somewhat larger scatter than found in Paper I. The flexible and somewhat subjective nature of the fitting procedure, compounded with the differences in the models, may account for the slightly higher age of the Yi et al. (2002) fit and the systematically lower moduli between $(m-M) = 10.00$ and 10.10.

To summarize, when analyzed in an internally consistent manner, the clusters NGC 752, IC 4651, and NGC 3680 have $E(B - V) = 0.03$, 0.10, and 0.06, respectively. The metallicities of NGC 752 and NGC 3680 are effectively the same and lie between $[\text{Fe}/\text{H}] = -0.10$ and -0.15 , on a scale where the Hyades and IC 4651 have $[\text{Fe}/\text{H}] = +0.12$. The respective apparent moduli for NGC 752, IC 4651, and NGC 3680 are 8.3, 10.2, and 10.2. Finally, the correct age sequence for the clusters, with the revised $[\text{Fe}/\text{H}]$ for NGC 3680, is 1.55, 1.7, and 1.85 Gyr, respectively, with a typical uncertainty of ± 0.1 Gyr. It should be noted that while one may quarrel with the absolute scale because of the choice of a particular set of isochrones, the relative rankings should be immune to changes other than in the reddening and/or the metallicity. Given these parameters, we now turn our attention to the giant branch.

5.4. The CMD: The Giant Branch and Li

While the turnoff regions and the luminosity of the clumps for NGC 752 and NGC 3680 are quite compatible, one is faced with the color discrepancy in the red giant clump: the clump for NGC 3680 is

almost 0.10 mag redder than in NGC 752. While theory predicts that the clump should generally shift toward the red with age for intermediate age clusters, the theoretical isochrones do not predict a change as large as that evidenced by NGC 752 and NGC 3680 for an age change of 0.3 Gyr (Girardi et al. 2000). However, the color difference is consistent with the shift between stars in the clump and the first-ascent red giant branch. In fact, the reddest star at clump level in NGC 752, usually assumed to be a first-ascent giant, is superposed within the clump of NGC 3680, while the bluer star in the clump of NGC 3680 is surrounded by the clump of NGC 752.

One interpretation is that the red giant region of NGC 752 is dominated by He-core-burning stars while that of NGC 3680 is dominated by first-ascent red giants. This isn't the first time this suggestion has been made. Pasquini et al. (2001) have measured Li abundances for an array of stars in NGC 3680 ranging from the tip of the giant branch to the fainter regions of the turnoff. The surprising result was that the majority of the stars in the clump (three out of four) have measurable Li with $\log(\text{Li}) + 12$ near 1.0. In contrast, the clump stars in NGC 752 have only upper limits at a factor of 5 or more below those in NGC 3680 and the stars classed as first-ascent giants in NGC 752. The effect is illustrated in Fig. 7 where we have plotted the Li abundance as a function of V for NGC 752 and NGC 3680 with the V magnitudes for NGC 3680 reduced by 1.90 to place them on the same scale. Upper limits are plotted as triangles, filled symbols refer to NGC 3680, open symbols to NGC 752. All stars, binaries or not, have been included in the figure. The bifurcation among the stars in the giant branch clump is relatively apparent. Note also the respectable match in V for the Li-dips on the main sequence. What is new in the analysis is the fact that the Li-bifurcation superposes on the color distribution of the giants, a fact previously lost due to the uncertainty in the metallicity of NGC 3680 relative to NGC 752. A significantly more metal-rich NGC 3680 would be expected to have a redder clump than NGC 752. With similar metallicity, the luminosity and color distribution should be almost identical.

In Fig. 8, we show the composite giant branch for NGC 752 (circles), IC 4651 (triangles), and NGC 3680 (squares). The photometry has been

corrected for reddening and distance and the points for IC 4651 have been reduced in color by an additional 0.01 mag in $b - y$ to partially correct for metallicity effects. The color index chosen for the temperature scale is $(b - y)$ due to its lower sensitivity to metallicity changes. As the clusters age, the color distribution of the stars near the clump shifts from primarily blue, mixed range of blue to red, to mostly red in NGC 3680. Though the majority of these stars have been analyzed for Li, only the filled symbols identify stars with measured $[\log(\text{Li}) + 12]$ of +1.0 or higher. With the exception of the fourth clump star in NGC 3680 with a Li abundance of +0.3, all other determinations are upper bounds. Of the 6 stars with definitive high values, three fall at the clump level in NGC 3680; the remaining three are spread out along the apparent path of the first-ascent giant branch.

If the giants in NGC 3680 are predominantly first-ascent giants, why do they simulate a clump? The distribution of first-ascent giants is partially controlled by the bump that results when the H-burning shell crosses the discontinuity in composition created by the deep limit of the convective atmosphere as the star ascends the giant branch. This discontinuity causes the star to retreat back down the giant branch and then reascend, creating a bump in the distribution due to the increased length of time spent in this luminosity range. Examples of this effect are seen in the giant tracks of Fig. 6. What is important to note is that the low-luminosity limit of the bump grows fainter as the mass of the star ascending the giant branch declines. For clusters younger than NGC 752, the bump stars are expected to lie above the level of the red giant clump; for clumps the age of NGC 3680 or higher, the bump approaches the same level as the clump created by the He-core burning stars. Thus, the possibility exists that the clump in NGC 3680 represents a totally different phase of evolution compared with the stars in NGC 752.

Why should the ratio of first-ascent to second-ascent giants change so dramatically? The only option we can offer comes from the one key parameter that changes as the clusters age from NGC 752 to NGC 3680, the drop in stellar mass. The stars that populate the giant branch are at the critical mass range where He-ignition changes from a quiescent phase to degenerate-core flash (Girardi et

al. 2000). The implication is that the development of the degenerate core and the evolution after ignition alter the luminosity function in a way that minimizes the He-core burning clump while coincidentally enhancing the bump at a luminosity comparable to the clump. The only other alternative that presents itself is that these relatively Li-rich stars are second-ascent giants, but the changeover in the internal structure severely reduces the rate of Li destruction in the post-main-sequence phase. The evidence available to date is inadequate to decide if either of these two options is correct. At minimum, it appears certain that standard stellar evolution does not predict this behavior among the giants in this age range. Because of the small number statistics, comprehensive observations of potential indicators of evolutionary states among giants, e.g., Li and C isotope ratios, for every cluster giant member of a number of clusters of very comparable age may be required ultimately to answer this new riddle.

6. Summary and Conclusions

Our understanding of NGC 3680 in the context of constraining stellar and galactic evolution has followed an uneven path, with grudging progress as successive studies have revised, clarified and added to previous work while leaving key questions unresolved. NGC 3680 ranked with NGC 752 (Twarog 1983) as one of the first clusters classified as having what was then described as a bimodal main sequence (Nissen 1988). The work of Nissen (1988) and Anthony-Twarog et al. (1989) refined the structure of the turnoff and collectively demonstrated via *uvby* photometry that the stars redward of the vertical turnoff in the CMD were probable members and unlikely binaries, identical to the pattern found in NGC 752. Recent work, including Nordström et al. (1996); Bruntt et al. (1999) and this study, has confirmed that this photometric spread in $b-y$ is real. Since standard stellar evolution models were incapable of producing single or binary stars with the appropriate redder colors at the turnoff, an alternative mechanism was necessary.

The suggestion that core convective overshoot could explain the peculiar CMD structure in NGC 3680 was first made by Mazzei & Pigatto (1988) and explicitly tested by Anthony-Twarog et al.

(1989) using the preliminary overshoot models of Bertelli et al. (1988). It was concluded that the red hook was naturally produced by single stars undergoing convective overshoot convolved with the normal binary sequence approximately 0.7 mag above the main sequence. Though the early attempts at creating isochrones with convective overshoot for stars in the intermediate-mass ranges were flawed, confirmation of this solution came through comprehensive identification of single-star members and binaries in an open cluster with the study of NGC 752 by Daniel et al. (1994) and the revised isochrones of Schaller et al. (1992). The same issue for NGC 3680 has been investigated periodically (Andersen et al. 1990; Carraro et al. 1993; Nordström et al. 1997; Kozhurina-Platais et al. 1997) as stellar models and the observational data for the cluster have improved. Despite the sparse population of the cluster and the rich population of binaries, the predominant debate that remains is not the existence of convective overshoot, but the required size of the phenomenon and its dependence on other factors such as metallicity. The necessity for the phenomenon again lies with the stars that define the red hook at the turnoff; proper motions and radial velocities have confirmed their original photometric classification as single-star members. The small population of these stars, however, limits the definition of the amount of overshoot unless the entire CMD is used, including the red giants, and the sample is enhanced by merger with clusters similar in age and metallicity, as in NGC 752 and IC 4651.

Unfortunately, for reasons discussed earlier, definitive values for the age were unattainable due to the controversy over the true metallicity. Estimates of the effect on the age of changing $[\text{Fe}/\text{H}]$ between the two camps were typically 25 % (Pasquini et al. 2001), though Kozhurina-Platais et al. (1997) split the difference by adopting a solar metallicity. With the metallicity issue resolved and the agreement between the giant branch and the turnoff confirmed, NGC 3680 has been placed on an internally consistent reddening, metallicity, age, and distance scale with NGC 752 and IC 4651. The combination of membership information with high quality photometry demonstrates that despite a modest difference in age and turnoff mass, the stars that define the clump in NGC 3680

are systematically redder than those in NGC 752, while the giants in IC 4651 appear to straddle both camps. The limited data from Li are consistent with the claim that the so-called clump stars in NGC 3680 are, in fact, likely to be first-ascent red giants, as originally suggested by Pasquini et al. (2001). Whether this suggestion holds up under greater scrutiny, only time and more definitive observational data will tell. However, as with the early discrepancies between observation and theory noted prior to the inclusion of convective overshoot, the cluster data are indicative of a real effect not predicted by the current standard models for post-main-sequence evolution.

We should like to acknowledge the helpful and constructive comments made by the referee. The progress in this project would not have been possible without the time made available by the TAC and the invariably excellent support provided by the staff at CTIO. The majority of the paper was completed during an extended visit to CTIO and the authors gratefully acknowledge the use of the facilities and the support received from the staff during this period. Suchitra Balachandran kindly communicated her results on Li in IC 4651 in advance of publication. Extensive use was made of the SIMBAD database, operating at CDS, Strasbourg, France and the WEBDA database maintained at the University of Geneva, Switzerland. The cluster project has been helped by support supplied through the General Research Fund of the University of Kansas and from the Department of Physics and Astronomy.

REFERENCES

- Andersen, J., Nordström, B., & Clausen, J. 1990, *ApJ*, 363, L33
- Andrievsky, S. M., Bersier, D., Kovtyukh, V. V., Luck, R. E., Maciel, W. J., Lépine, J. R. D., & Beletsky, Yu. V. 2002a, *A&A*, 384, 140
- Andrievsky, S. M., Kovtyukh, V. V., Luck, R. E., Lépine, J. R. D., Maciel, W. J., & Beletsky, Yu. V. 2002b, *A&A*, 392, 491
- Anthony-Twarog, B. J. 1987a, *AJ*, 93, 647
- Anthony-Twarog, B. J. 1987b, *AJ*, 93, 1454
- Anthony-Twarog, B. J., Heim, E. A., Twarog, B. A., & Caldwell, N. 1991a, *AJ*, 102, 1056
- Anthony-Twarog, B. J., Laird, J. B., Payne, D., & Twarog, B. A. 1991b, *AJ*, 101, 1922
- Anthony-Twarog, B. J., Sarajedini, A., Twarog, B. A., & Beers, T. C. 2000, *AJ*, 119, 2882
- Anthony-Twarog, B. J., & Twarog, B. A. 1987, *AJ*, 94, 1222
- Anthony-Twarog, B. J., & Twarog, B. A., 1998, *AJ*, 116, 1902
- Anthony-Twarog, B. J., & Twarog, B. A. 2000a, *AJ*, 119, 2282 (Paper I)
- Anthony-Twarog, B. J., & Twarog, B. A. 2000b, *AJ*, 120, 3111 (Paper II)
- Anthony-Twarog, B. J., Twarog, B. A., & Craig, J. 1995, *PASP*, 107, 32
- Anthony-Twarog, B. J., Twarog, B. A., & Sheeran, M. 1994, *PASP*, 106, 486
- Anthony-Twarog, B. J., Twarog, B. A., & Shodhan, S. 1989, *AJ*, 98, 1634
- Anthony-Twarog, B. J., Twarog, B. A., & Yu, J. 2002, *AJ*, 124, 389
- Baird, S. R. 1996, *AJ*, 112, 2132
- Bertelli, G., Bressan, A. G., Chiosi, C., Nasi, E., & Pigatto, L. 1988, preprint
- Bruntt, H., Frandsen, S., Kjeldsen, H., & Andersen, M. I. 1999, *A&AS*, 140, 135
- Carraro, G., Bertelli, G., Bressan, A., & Chiosi, C. 1993, *A&AS*, 101, 381
- Chaboyer, B., Deliyannis, C. P., Demarque, P., Pinsonneault, M. H., & Sarajedini, A. 1992, *ApJ*, 388, 372
- Clariá, J. J., & Lapasset, E. 1983, *JApA*, 4, 117
- Corder, S., & Twarog, B. A. 2001, *AJ*, 122, 895
- Crawford, D. L. 1975, *AJ*, 80, 955
- Crawford, D. L., & Barnes, J. V. 1970, *AJ*, 75, 946
- Daniel, S. A., Latham, D. W., Mathieu, R. D., & Twarog, B. A. 1994, *PASP*, 106, 281

- Edvardsson, B., Andersen, J., Gustaffson, B., Lambert, D. L., Nissen, P. E., & Tomkin, J. 1993, *A&A*, 275, 101
- Eggen, O. J. 1969, *ApJ*, 155, 439
- Eggen, O. J. 1983, *AJ*, 88, 813
- Eggen, O. J. 1989, *PASP*, 101, 366
- Friel, E. D., & Janes, K. A. 1993, *A&A*, 267, 75
- Friel, E. D., Janes, K. A., Tavaréz, M., Scott, J., Hong, L., & Miller, N. 2002, *AJ*, 124, 2693
- Geisler, D., Claria, J. J., & Minniti, D. 1991, *AJ*, 102, 1836
- Girardi, L., Mermilliod, J. -C., & Carraro, G. 2000, *A&A*, 354, 892
- Girardi, L. et al. 2002, *A&A*, 391, 195
- Green, E. M., Demarque, P., & King, C. R. 1987, Revised Yale Isochrones and Luminosity Functions (Yale University Observatory, New Haven)
- Harris, G. L. H., FitzGerald, M. P. V., Mehta, S. & Reed, B. C. 1993, *AJ*, 106, 1533
- Hawley, S. L., Tourtellot, J. G., & Reid, I. N. 1999, *AJ*, 117, 1341
- Janes, K. A. 1977, *AJ*, 82, 35
- Janes, K. A. 1979, *ApJS*, 39, 135
- Kozhurina-Platais, V., Demarque, P., Platais, I., Orosz, J. A., & Barnes, S. 1997, *AJ*, 113, 1045
- Kozhurina-Platais, V., Girard, M., Platais, I., & Van Altena, W. F. 1995, *AJ*, 109, 672
- Lépine, J. R. D., Acharova, I. A., & Mishurov, Yu. N. 2003, *ApJ*, 589, 210
- Luck, R. E., Gieren, W. P., Andrievsky, S. M., Kovtyukh, V. V., Fouqué, P., Pont, F., & Kienzle, F. 2003, *A&A*, 401, 939
- Mazzei, P., & Pigatto, L. 1988, *A&A*, 193, 148
- McClure, R. D. 1972, *ApJ*, 172, 615
- Meibom, S. 2000, *A&A*, 361, 929
- Meibom, S., Andersen, J., & Nordström 2002, *A&A*, 386, 187
- Mermilliod, J. -C., Andersen, J., Nordström, B., & Mayor, M. 1995, *A&A*, 299, 53
- Mishurov, Yu. N., Lépine, J. R. D., & Acharova, I. A. 2002, *ApJ*, 571, L113
- Nissen, P. E. 1988, *A&A*, 199, 146
- Nissen, P. E., Twarog, B. A., & Crawford, D. L. 1987, *AJ*, 93, 634
- Nordström, B., Andersen, J., & Andersen, M. I. 1996, *A&AS*, 118, 407
- Nordström, B., Andersen, J., & Andersen, M. I. 1997, *A&A*, 322, 460
- Olsen, E. H. 1983, *A&AS*, 54, 55
- Olsen, E. H. 1988, *A&A*, 189, 173
- Olsen, E. H. 1993, *A&AS*, 102, 89
- Olsen, E. H. 1994, *A&AS*, 106, 257
- Pasquini, L., Randich, S., & Pallavicini, R. 2001, *A&A*, 375, 851
- Schaller, G., Schaerer, D., Meynet, G., & Maeder, G. 1992, *A&AS*, 96, 269
- Schlegel, D. J., Finkbeiner, D. P., & Davis, M. 1998, *ApJ*, 500, 525
- Schuster, W. J., & Nissen, P. E. 1989, *A&A*, 221, 65
- Shobbrook, R. R. 1985, *MNRAS*, 212, 591
- Snowden, M. S. 1975, *PASP*, 87, 721
- Twarog, B. A. 1983, *ApJ*, 267, 207
- Twarog, B. A., & Anthony-Twarog 1989, *AJ*, 97, 759
- Twarog, B. A., & Anthony-Twarog, B. J. 1995, *AJ*, 109, 2828
- Twarog, B. A., & Anthony-Twarog, B. J. 1996, *AJ*, 112, 1500
- Twarog, B. A., Anthony-Twarog, B. J., & Bricker, A. R. 1999, *AJ*, 117, 1816

Twarog, B. A., Anthony-Twarog, B. J., & De Lee,
N. M. 2003, AJ, 125, 1383 (Paper III)

Twarog, B. A., Anthony-Twarog, B. J., & Hawar-
den, T. G. 1995, PASP, 107, 1215

Twarog, B. A., Anthony-Twarog, B. J., & Mc-
Clure, R. D. 1993, PASP, 105, 78

Twarog, B. A., Ashman, K. M., & Anthony-
Twarog, B. A. 1997, AJ, 114, 2556

Yi, S. K., Kim, Y. -C, & Demarque, P. 2002, ApJS,
144, 259

Fig. 1.— Standard errors of the mean for V , and all color indices as a function of V . Major tick-marks for the y axis are 0.05 apart. The vertical scale for each successive index has been offset by 0.05 mag for visual clarity.

Fig. 2.— Color-magnitude diagram for stars with at least 2 observations each in b and y . Crosses are stars with internal errors in $b - y$ greater than 0.010 mag.

Fig. 3.— CMD for stars at the turnoff with errors in $b - y$ below 0.011 mag. Crosses are stars selected as field stars blueward of the main sequence while triangles are probable field stars and/or binaries above the main sequence.

Fig. 4.— CMD for the same stars as Fig. 3, using $u - y$ as the temperature index.

Fig. 5.— CMD of all potential members of NGC 3680 superposed on the CMD for NGC 752. Filled triangles are probable binaries in NGC 3680 while filled circles are all other stars. Asterisks are probable binaries in NGC 752 while open circles are all other stars. The data in NGC 3680 is shifted by -0.03 in $B - V$ and -1.90 in V .

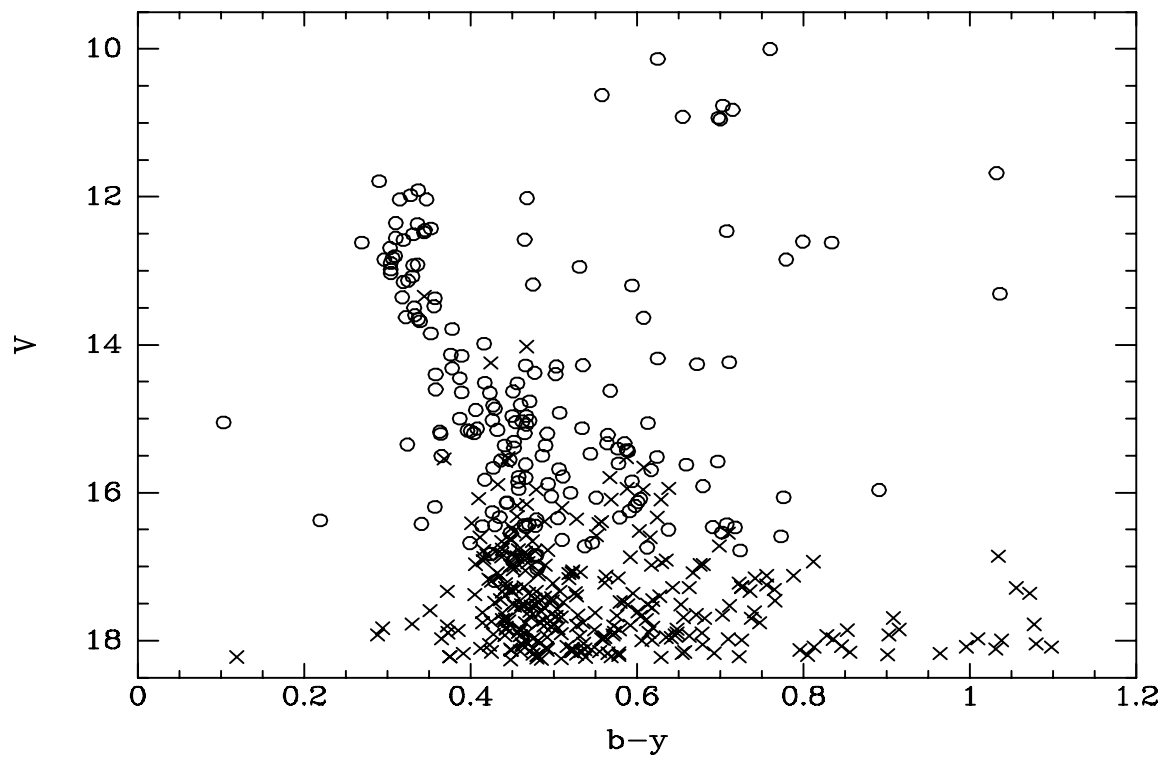
Fig. 6.— Same data as Fig. 5 with binaries in NGC 752 removed and all stars in NGC 3680 drawn as filled circles. Isochrones have solar abundance and have been corrected for reddening and distance by $E(B - V) = 0.03$ and $(m - M) = 8.50$.

Fig. 7.— Li abundance measures in NGC 752 (open symbols) and NGC 3680 (filled symbols) as a function of V with NGC 3680 at the same distance and reddening as NGC 752. Triangles are upper limits.

Fig. 8.— Composite absolute CMD for all the giants in NGC 752 (circles), IC 4651 (triangles), and NGC 3680 (squares). Filled symbols are all stars with measured $\log(\text{Li}) + 12$ above +1.0.

TABLE 1. Photoelectric *Caby* Photometry of NGC 3680 Stars

ID	V	σ_V	$b - y$	σ_{by}	hk	σ_{hk}	N
11	10.925	0.009	0.653	0.004	1.124	0.006	5
20	10.151	0.011	0.625	0.007	1.076	0.006	5
26	10.946	0.008	0.698	0.002	1.223	0.004	4
27	10.779	0.002	0.703	0.004	1.253	0.012	4
29	11.982	0.000	0.339	0.000	0.519	0.000	1
34	10.631	0.007	0.561	0.004	0.775	0.003	4
41	10.926	0.010	0.695	0.002	1.227	0.009	4
54	8.904	0.000	0.735	0.000	1.421	0.000	1



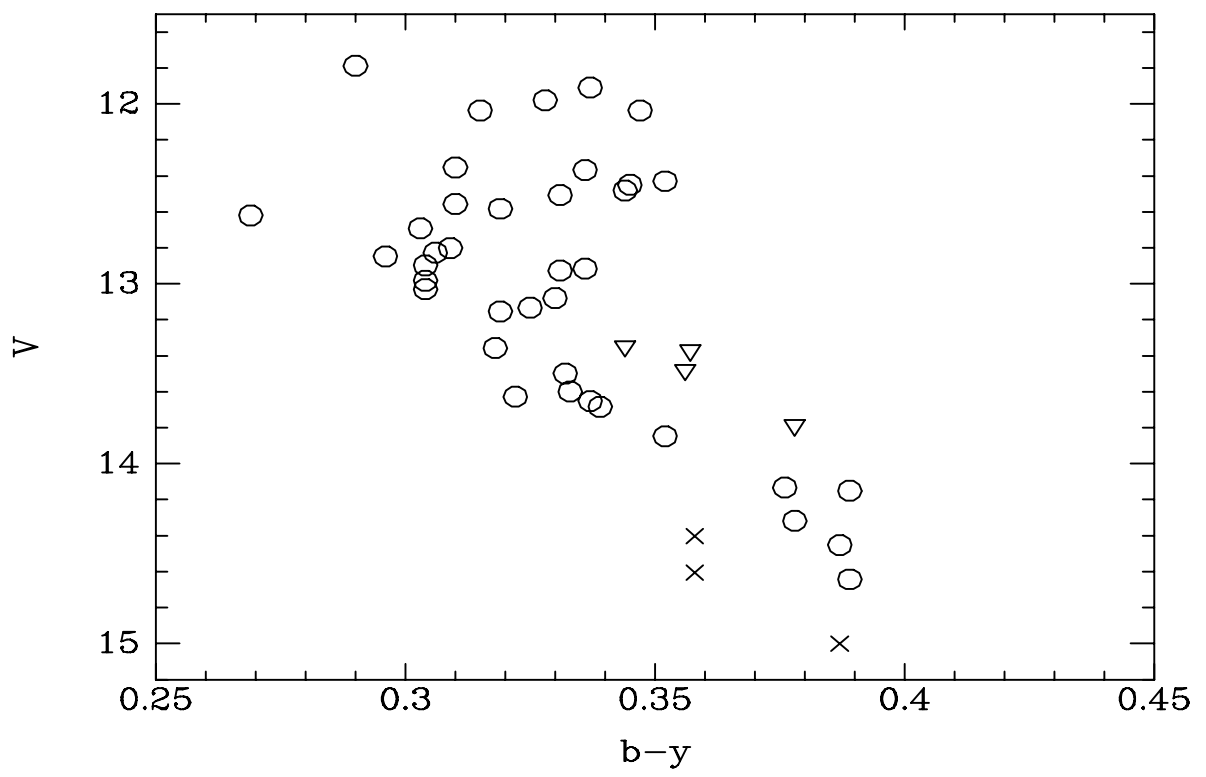


TABLE 3. Photometric Comparisons : Table 2 - Reference

$\Delta(V)$	s.e.m.	$\Delta(b - y)$	s.e.m.	N	Limits	Excluded Stars	References
0.005	0.023	0.004	0.026	79	$V < 17$	20, 84, 2054	Anthony-Twarog et al. (1989)
0.010	0.014	0.007	0.013	43	$V < 15$	20, 84	Anthony-Twarog et al. (1989)
0.025	0.032	0.005	0.030	137	$V < 17$		Bruntt et al. (1999)
0.014	0.018	0.006	0.013	61	$V < 15$		Bruntt et al. (1999)
0.029	0.029	0.016	0.023	200	$V < 17$	511,527	Nordström et al. (1996)
0.000	0.026	0.000	0.019	200	$V < 17$	511,527	Corrected for color term
0.020	0.022	0.017	0.019	86	$V < 15$		Nordström et al. (1996)
0.000	0.017	0.000	0.010	86	$V < 15$		Corrected for color term

Notes to Table 3.

$$V(\text{Table2}) = V(\text{NOR}) + 0.094 * (b - y) - 0.021; b - y(\text{Table2}) = 1.108 * (b - y)(\text{NOR}) - 0.031$$

